Available online at www.sciencedirect.com
SCIENCE DIRECT
Journal of Sound and Vibration 295 (2006) 282–293
JOURNAL OF SOUND AND VIBRATION
www.elsevier.com/locate/jsvi

Modeling study of a flexible hub–beam system with large motion and with considering the effect of shear deformation

You Chaolan*, Hong Jiazhen, Cai Guoping

Department of Engineering Mechanics, Shanghai Jiaotong University, Shanghai 200240, China

Received 6 December 2004; received in revised form 22 July 2005; accepted 14 January 2006
Available online 29 March 2006

Abstract

For a flexible hub–beam system with large motion, the first-order approximation coupling (FOAC) model is developed currently, which is verified numerically and experimentally to be valid for dynamic description of the system. In the FOAC model, the assumption of Euler–Bernoulli beam is adopted with neglecting the effect of shear deformation of flexible beam. So this model is only available for the case of slender beam. When the beam is short in length direction, shear deformation is a factor that may have biggish effect on system dynamics.

In this paper, dynamic modeling of flexible hub–beam system with considering the effect of shear deformation is investigated. Firstly, based on the assumption of Timoshenko beam and using Hamilton's principle, a coupling dynamic model with considering shear deformation is established, in which geometric stiffness term and axial foreshortening effect caused by the transverse deformation of beam are considered in the modeling. Subsequently, the dynamic model is discretized using finite element method (FEM). Finally numerical simulations are carried out to demonstrate the effectiveness of proposed dynamic model. Simulation results indicate that, dynamics characteristics of the hub–beam system using the Timshenko beam hypothesis and the Euler–Bernoulli beam hypothesis are almost identical when the beam is a slender one. For this case, shear deformation has little effect on system dynamics. But when the beam is short in length direction, shear deformation may have biggish effect on system dynamics. This effect becomes larger as the width to length ratio increases.

1. Introduction

It is well known that flexible multi-body systems with large motion have many applications in many practical engineering, such as aeronautics, aerospace and robotics, where a flexible hub–beam system is a typical one. A good dynamic model for flexible hub–beam system is essentially important in many engineering applications, such as satellite antennas, helicopter blades, and robot manipulators.

For a flexible hub–beam system, the traditional modeling theory adopts small deformation assumption in structural dynamics, which thinks that the axial and transverse deformations at any point in the beam are uncoupled, namely linear deformation field of flexible beam is adopted. The dynamic model established based

*Corresponding author.
E-mail address: ycl_sjtu@hotmail.com (Y. Chaolan).

0022-460X/$ - see front matter © 2006 Published by Elsevier Ltd.
doi:10.1016/j.jsv.2006.01.047

on this linear deformation field by using the hybrid coordinate method is the so-called hybrid coordinate model, i.e. the zeroth-order approximation coupling (ZOAC) model [1,2]. In 1987 Kane et al. [3] investigated a rotating flexible cantilever beam using the ZOAC model and showed that this model failed to describe the dynamic behavior of beam when the beam is in high rotation speed. The dynamic stiffening phenomenon was first pointed out [3]. Since then, most studies on rigid–flexible coupling dynamic systems are focused on the investigation of dynamic stiffening and many methodologies are developed to capture the dynamic stiffening term in the dynamic systems [4–6]. The introduction of dynamic stiffening indicates that there still exist big limitations on the understanding of dynamics mechanism of rigid–flexible coupling systems, and on the accuracy of the mathematical model established to describe the dynamic behavior of the systems. Meanwhile, it also promotes extensive research on the modeling of the rigid–flexible coupling dynamic systems.

Recently, based on the theory of continuum medium mechanics and the theory of analysis dynamics, and with the consideration of the second-order coupling term of axial displacement caused by the transverse displacement of the flexible beam, the first-order approximation coupling (FOAC) model is developed [7–14]. The physical explanation to the dynamic stiffening is suggested in Ref. [12] by using the FOAC model. The dynamic stiffening is essentially a structural dynamic problem in non-inertial system, which results from the additional stiffness caused by the coupling of large rotation motion and small elastic vibration of the flexible beam [12]. In addition, the existence of dynamic stiffening and the validity of the FOAC model are experimentally verified in Refs. [12–14]. The FOAC model is available for low rotation speed and high rotation speed as well. However, in the studies [7–14], the Euler–Bernoulli hypothesis is adopted for flexible beam and the effect of shear deformation of the flexible beam is neglected in the modeling. There has result indicating that [15], when the beam is short in length direction, shear deformation of the beam will have biggish effect on system dynamics and should be considered in the modeling. Therefore, it is essential to study dynamics modeling of the hub–beam system with considering the shear deformation, and make comparison studies between the results using the Timoshenko beam hypothesis and those using the Euler–Bernoulli beam hypothesis.

In this paper, modeling of a flexible hub–beam with considering the effect of shear deformation is studied. Geometric stiffness terms and axial foreshortening effect caused by the transverse deformation of the beam are considered in the modeling. The results using the Timoshenko beam hypothesis are compared with those using the Euler–Bernoulli beam hypothesis. This paper is organized as follows. Section 2 presents the expression of dynamic model of flexible hub–beam by Hamilton's principle and using finite element method (FEM) for discretization. Numerical simulations are presented in Section 3. A concluding remark is given in Section 4.

2. Motion equation

The structural model of a flexible hub–beam system is shown in Fig. 1. The hub is rigid body and its radius is represented by R. The flexible beam is attached to the hub at the point O. The properties of the flexible beam are represented as follows. The parameter L is the length of the beam; A is the cross section area; I is the area

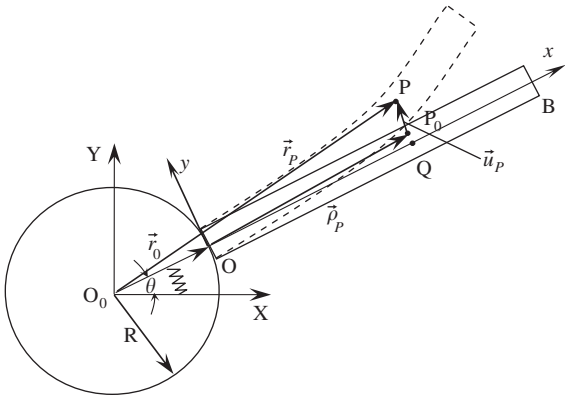

Fig. 1. Structural model of a flexible hub–beam system.

moment of inertia of the beam cross section; ρ is the mass per unit volume; E is the Young's modulus of the beam material. It is assumed that a coiling spring is placed on the hub, as shown in Fig. 1. The system moves in the XY plane and the effect of gravity is neglected. Two coordinate systems, an inertial frame O_0–XY and a reference frame O–xy, are used, as shown in Fig. 1. The point P_0 is an arbitrary point in the beam, and Q is the corresponding point of P_0 on the centroid axis. After deformation the point P_0 moves to the point P. The vector of the point P in the O_0-XY frame may be written as

$$\vec{r}_P = \vec{r}_0 + \vec{\rho}_P + \vec{u}_P \tag{1}$$

where $\vec{r}_0 = \overrightarrow{O_0O}$, $\vec{\rho}_P = \overrightarrow{OP_0}$ and $\vec{u}_P = \overrightarrow{P_0P}$ is the deformation vector. The coordinates of $\vec{r}_P$ and $\vec{r}_0$ in the O_0-XY frame are represented by $\mathbf{r}_P$ and $\mathbf{r}_0$, and that of $\vec{\rho}_P$ and $\vec{u}_P$ in the O–xy frame by $\boldsymbol{\rho}_P$ and $\mathbf{u}_P$, respectively. The parameter $\boldsymbol{\Theta}$ is a direction cosine matrix which is the O–xy frame with respect to the O_0–XY frame, given by

$$\boldsymbol{\Theta} = \begin{bmatrix} \cos\theta & -\sin\theta \\ \sin\theta & \cos\theta \end{bmatrix}, \tag{2}$$

where θ is the angular displacement of the hub. The coordinate of the point O in the O_0–XY frame may be written as

$$\mathbf{r}_0 = \boldsymbol{\Theta}\begin{bmatrix} R \\ 0 \end{bmatrix} = \begin{bmatrix} R\cos\theta \\ R\sin\theta \end{bmatrix}. \tag{3}$$

The coordinate of $\vec{r}_P$ in the O_0–XY frame may be written as

$$\mathbf{r}_P = \mathbf{r}_0 + \boldsymbol{\Theta}(\boldsymbol{\rho}_P + \mathbf{u}_P), \tag{4}$$

where $\boldsymbol{\rho}_P = [x, y]^{\mathrm{T}}$ and $\mathbf{u}_P = [u, v]^{\mathrm{T}}$, as shown in Fig. 2. The variables x and y are the coordinates of the point P_0 in the O–xy frame; u and v are the deformation quantities of the point P_0 in x direction and y direction in the O–xy frame, respectively. Since v is much larger than u, it is reasonable to assume that the deformation quantity of P_0 in y direction is equal to that of Q in y direction.

In consideration of the axial foreshortening quantity caused by the transverse deformation of beam, u may be written as

$$u = u_s - y\phi + u_f, \tag{5}$$

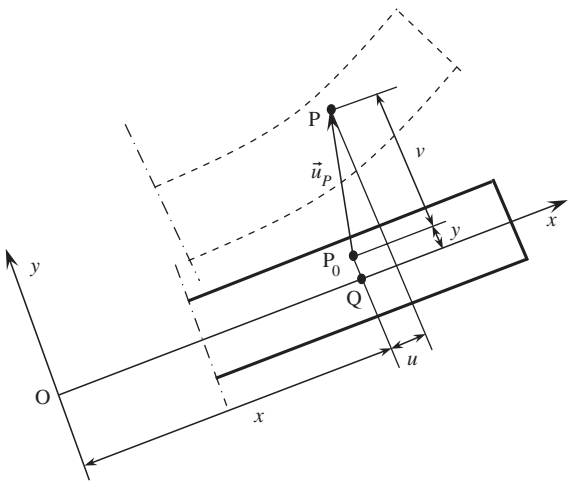

Fig. 2. Schematic diagram of deformation of flexible beam.

where u_s is the axial stretching quantity of the point Q; ϕ is the angular displacement of cross section; and u_f is the deformation associated with the foreshortening quantity, given by [7–14]

$$u_f = -\frac{1}{2}\int_0^x \left(\frac{\partial v}{\partial \xi}\right)^2 \mathrm{d}\xi. \tag{6}$$

Substituting Eqs. (3), (5) and (6) into Eq. (4), we have

$$\mathbf{r}_P = \mathbf{\Theta}\begin{bmatrix} R + x + u_s - y\phi - \frac{1}{2}\int_0^x \left(\frac{\partial v}{\partial \xi}\right)^2 \mathrm{d}\xi \\ y + v \end{bmatrix}, \tag{7}$$

The first-order derivative of $\mathbf{r}_p$ may be expressed as

$$\dot{\mathbf{r}}_P = \mathbf{\Theta}\tilde{\mathbf{I}}\begin{bmatrix} R + x + u_s - y\phi + u_f \\ y + v \end{bmatrix}\dot{\theta} + \mathbf{\Theta}\begin{bmatrix} \dot{u}_s - y\dot{\phi} + \dot{u}_f \\ \dot{v} \end{bmatrix}, \tag{8}$$

where

$$\tilde{\mathbf{I}} = \begin{bmatrix} 0 & -1 \\ 1 & 0 \end{bmatrix}, \tag{9}$$

$$\dot{u}_f = -\int_0^x \frac{\partial v}{\partial \xi}\cdot\frac{\partial \dot{v}}{\partial \xi}\,\mathrm{d}\xi. \tag{10}$$

The kinetic energy of the hub–beam system is written as

$$T = T_H + T_B = \frac{1}{2}J_H\dot{\theta}^2 + \frac{1}{2}\int_V \rho\dot{\mathbf{r}}_P^{\mathrm{T}}\dot{\mathbf{r}}_P\,\mathrm{d}V, \tag{11}$$

where T_H and T_B are the kinetic energy of the hub and the flexible beam, respectively; J_H is the rotary inertia of the hub.

Next consider the potential energy of the system. Using a nonlinear strain–displacement relationship, the axial normal strain of the beam may be expressed as

$$\varepsilon_x = \frac{\partial u}{\partial x} + \frac{1}{2}\left(\frac{\partial v}{\partial x}\right)^2. \tag{12}$$

Substituting Eq. (5) into Eq. (12), we have

$$\varepsilon_x = \frac{\partial u_s}{\partial x} - y\frac{\partial \phi}{\partial x}. \tag{13}$$

The axial normal stress of the beam, σ_x, may be written as

$$\sigma_x = E\varepsilon_x. \tag{14}$$

The shear stress of cross section of the beam, τ, may be written as

$$\tau = \kappa G\alpha, \tag{15}$$

where α is the shear angle; κ is the shear coefficient of cross section; and G is the shear modulus, given by $G = E/2(1+\mu)$, where μ is Poisson's ratio. The parameter α may be expressed as

$$\alpha = \phi - \frac{\partial v}{\partial x}. \tag{16}$$

The potential energy of the system may be written as

$$U = U_C + U_f = \frac{1}{2}k_C\theta^2 + \frac{1}{2}\left(\int_V \sigma_x\varepsilon_x\,\mathrm{d}V - \int_V \tau\alpha\,\mathrm{d}V\right), \tag{17}$$

where U_C and U_f are the potential energy of the coiling spring and the flexible beam, respectively; k_C is the stiffness coefficient of the coiling spring. Using Eqs. (13)–(16), the potential energy of the flexible beam may be

written as

$$U_f = \frac{1}{2}\int_0^L EA\left(\frac{\partial u_s}{\partial x}\right)^2 \mathrm{d}x + \frac{1}{2}\int_0^L EI\left(\frac{\partial \phi}{\partial x}\right)^2 \mathrm{d}x + \frac{1}{2}\int_0^L \kappa GA\left(\phi - \frac{\partial v}{\partial x}\right)^2 \mathrm{d}x. \tag{18}$$

From Eqs. (11) and (17), the variation δT and δU can be computed. Assuming that the external force vector $\mathbf{f}$ acted on the beam is the distribute force. The coordinate of $\mathbf{f}$ in the O–xy frame is represented by $\mathbf{f} = [f_1, f_2]^{\mathrm{T}}$. So the coordinate of $\mathbf{f}$ in the O_0–XY frame is given by $\mathbf{\Theta f}$. The virtual work by the external force may be written as

$$\delta W = \int_0^L (\mathbf{\Theta f})^{\mathrm{T}} \delta \mathbf{r}_P \, \mathrm{d}x. \tag{19}$$

Using the Hamilton's principle $\delta H = \int_{t_1}^{t_2} (\delta T - \delta U + \delta W)\,\mathrm{d}t = 0$, the dynamic equations of the system in partial differential form may be obtained as

$$\begin{aligned} &J_H\ddot{\theta} + \int_0^L \rho A\Big\{\ddot{\theta}\Big[\big(R + x + u_s + u_f\big)^2 + v^2\Big] + \big(R + x + u_s + u_f\big)\ddot{v} - v\big(\ddot{u}_s + \ddot{u}_f\big) \\ &+2\dot{\theta}\Big[\big(R + x + u_s + u_f\big)\big(\dot{u}_s + \dot{u}_f\big) + v\dot{v}\Big]\Big\}\,\mathrm{d}x + \int_0^L \rho I\Big[\ddot{\theta}\big(1 + \phi^2\big) + \ddot{\phi} + 2\phi\dot{\phi}\dot{\theta}\Big]\,\mathrm{d}x = F_\theta, \end{aligned} \tag{20}$$

$$\int_0^L \rho A\Big[-v\ddot{\theta} + \big(\ddot{u}_s + \ddot{u}_f\big) - \big(R + x + u_s + u_f\big)\dot{\theta}^2 - 2\dot{v}\dot{\theta}\Big]\,\mathrm{d}x - \int_0^L EA\frac{\partial^2 u_s}{\partial x^2} = F_u, \tag{21}$$

$$\int_0^L \rho I\Big\{\ddot{\theta} + \ddot{\phi} - \phi\dot{\theta}^2\Big)\,\mathrm{d}x - \int_0^L EI\frac{\partial^2 \phi}{\partial x^2} + \int_0^L \kappa GA\left(\phi - \frac{\partial v}{\partial x}\right)\mathrm{d}x = F_\phi, \tag{22}$$

$$\begin{aligned} &\int_0^L \rho A\Big\{\ddot{\theta}\big(R + x + u_s + u_f\big) + \ddot{v} - v\dot{\theta}^2 + 2\dot{\theta}\big(\dot{u}_s + \dot{u}_f\big) \\ &\quad + \frac{\partial}{\partial x}\left[\frac{\partial v}{\partial x}\cdot\int_x^L B(\xi, t)\,\mathrm{d}\xi\right]\Big\}\,\mathrm{d}x + \int_0^L \kappa GA\left(\frac{\partial \phi}{\partial x} - \frac{\partial^2 v}{\partial x^2}\right)\mathrm{d}x = F_v \end{aligned} \tag{23}$$

where F_θ, F_u, F_ϕ and F_v are the generalized external forces with respect to θ, u_s, ϕ and v, respectively. These four parameters and the parameter $B(x, t)$ in Eq. (23) can be expressed as

$$F_\theta = K_C\theta + \int_0^L A\big[f_2\big(R + x + u_s + u_f\big) - f_1 v\big]\,\mathrm{d}x, \tag{24}$$

$$F_u = \int_0^L A f_1\,\mathrm{d}x, \tag{25}$$

$$F_\phi = 0, \tag{26}$$

$$F_v = \int_0^L A\left[f_2 + \frac{\partial}{\partial x}\left(\frac{\partial v}{\partial x}\cdot\int_x^L f_1\,\mathrm{d}\xi\right)\right]\mathrm{d}x, \tag{27}$$

$$B(x, t) = \ddot{u}_s + \ddot{u}_f - v\ddot{\theta} - \dot{\theta}^2\big(R + x + u_s + u_f\big) - 2\dot{v}\dot{\theta}. \tag{28}$$

The boundary conditions of the beam are as follows:

$$\begin{gathered} u_s(0, t) = 0, \quad \phi(0, t) = 0, \quad u_f(0, t) = 0, \\ EA\frac{\partial u_s(L, t)}{\partial x} = 0, \quad EI\frac{\partial \phi(L, t)}{\partial x} = 0, \quad EI\frac{\partial^2 \phi(L, t)}{\partial x^2} = 0. \end{gathered} \tag{29}$$

The system dynamics given in Eqs. (20)–(23) are partial differential equations that are nonlinear and time-varying. It is generally impossible to get the analytical solutions of these equations. The FEM is often used as

discretization of the beam. Assume that the elastic beam is partitioned with n elements when using FEM. So the total number of the nodes of the beam is $(n+1)$. The finite element model of the flexible beam is shown in Fig. 3. The length of the ith element is represented by l_i. The $\bar{o}-\bar{x}\,\bar{y}$ system is the element coordinates system of the ith element. The position of $\bar{o}-\bar{x}\,\bar{y}$ system is determined by the coordinate x_i, which is the position of the first node of the ith element in the O–xy frame. The parameters u_s, ϕ and v are expressed as the interpolation of the two node coordinates of this element by using element shape function, given by

$$u_s(\bar{x},t)=\mathbf{N}_{i,1}(\bar{x})\ \mathbf{p}_i(t), \tag{30}$$

$$v(\bar{x},t)=\mathbf{N}_{i,2}(\bar{x})\ \mathbf{p}_i(t), \tag{31}$$

$$\phi(\bar{x},t)=\mathbf{D}_i(\bar{x})\ \mathbf{p}_i(t), \tag{32}$$

where $\bar{x}$ is the axial coordinate of point P in the $\bar{o}-\bar{x}\,\bar{y}$ system, as shown in Fig. 3. The variables $\mathbf{N}_{i,1}$, $\mathbf{N}_{i,2}$, and $\mathbf{D}_i$ are (1×6) vectors which are the iso-parametric shape function vectors of the ith element, and $\mathbf{p}_i$ is the (6×1) node coordinate vector, given by

$$\mathbf{N}_{i,1}(\bar{x})=\begin{bmatrix}N_{11} & 0 & 0 & N_{12} & 0 & 0\end{bmatrix}, \tag{33}$$

$$\mathbf{N}_{i,2}(\bar{x})=\begin{bmatrix}0 & N_{21} & N_{31} & 0 & N_{22} & N_{32}\end{bmatrix}, \tag{34}$$

$$\mathbf{D}_i(\bar{x})=\begin{bmatrix}0 & D_{21} & D_{31} & 0 & D_{22} & D_{32}\end{bmatrix}, \tag{35}$$

$$\mathbf{p}_i(t)=\begin{bmatrix}w_{1,i} & w_{2,i} & \phi_i & w_{1,i+1} & w_{2,i+1} & \phi_{i+1}\end{bmatrix}, \tag{36}$$

respectively, where [17]

$$\begin{gathered}
N_{11}=1-\zeta,\quad N_{21}=\frac{1}{1+\varphi}\left(1+\varphi-\varphi\zeta-3\zeta^2+2\zeta^3\right),\\
N_{12}=\zeta,\quad N_{22}=\frac{l_i}{1+\varphi}\left[\left(1+\frac{\varphi}{2}\right)\zeta-\frac{4+\varphi}{2}\zeta^2+\zeta^3\right],\\
N_{31}=\frac{1}{1+\varphi}\left(\varphi\zeta+3\zeta^2-2\zeta^3\right),\quad N_{32}=\frac{l_i}{1+\varphi}\left(-\frac{\varphi}{2}\zeta+\frac{\varphi-2}{2}\zeta^2+\zeta^3\right),\\
D_{21}=-\frac{6}{(1+\varphi)l_i}\left(\zeta-\zeta^2\right),\quad D_{22}=\frac{1}{1+\varphi}\left[1+\varphi-(4+\varphi)\zeta+3\zeta^2\right],\\
D_{31}=\frac{6}{(1+\varphi)l_i}\left(\zeta-\zeta^2\right),\quad D_{32}=\frac{1}{1+\varphi}\left((\varphi-2)\zeta+3\zeta^2\right),
\end{gathered} \tag{37}$$

where $\zeta=\bar{x}/l_i$. The parameter φ is the shear coefficient, given by $\varphi=12EI/\kappa GAl_i^2$. The variables $w_{1,i}$, $w_{2,i}$ and ϕ_i are the axial displacement, the transverse displacement and the cross-section rotation angle of the ith node, respectively, $i=1\sim(n+1)$.

The total generalized coordinate vector of the beam is represented by $\mathbf{p}(t)$, which is a $3(n+1)\times 1$ vector, given by

$$\mathbf{p}(t)=[\,w_{11}\quad w_{21}\quad \phi_1\quad \cdots\quad w_{1n+1}\quad w_{2n+1}\quad \phi_{n+1}\,]^{\mathrm{T}} \tag{38}$$

Thus the node coordinate vector $\mathbf{p}_i$ of the ith element may be written as

$$\mathbf{p}_i(t)=\mathbf{B}_i\mathbf{p}(t), \tag{39}$$

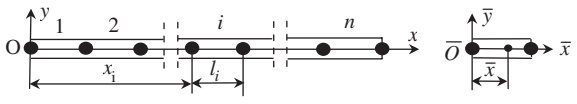

Fig. 3. Finite element model of flexible beam.

where $\mathbf{B}_i$ is a $6 \times 3(n+1)$ Boole indicated matrix that is determined by the element serial number as

$$\mathbf{B}_i = \begin{bmatrix} \mathbf{0}_3 & \mathbf{0}_3 & \cdots & \mathbf{I}_3 & \mathbf{0}_3 & \cdots & \mathbf{0}_3 & \mathbf{0}_3 \\ \mathbf{0}_3 & \mathbf{0}_3 & \cdots & \mathbf{0}_3 & \mathbf{I}_3 & \cdots & \mathbf{0}_3 & \mathbf{0}_3 \end{bmatrix}_{6\times 3(n+1)}, \tag{40}$$

where $\mathbf{0}_3$ is a (3×3) zero matrix and $\mathbf{I}_3$ is a (3×3) identity matrix. Substituting Eq. (39) into Eqs. (30)–(32), we have

$$u_s(\bar{x}, t) = \mathbf{N}_1(\bar{x})\ \mathbf{p}(t), \tag{41}$$

$$v(\bar{x}, t) = \mathbf{N}_2(\bar{x})\ \mathbf{p}(t), \tag{42}$$

$$\phi(\bar{x}, t) = \mathbf{D}(\bar{x})\ \mathbf{p}(t), \tag{43}$$

where $\mathbf{N}_1(\bar{x})$, $\mathbf{N}_2(\bar{x})$ and $\mathbf{D}(\bar{x})$ are all $1 \times 3(n+1)$ vector which are the shape function in the O–xy frame, given by $\mathbf{N}_1(\bar{x}) = \mathbf{N}_{i,1}(\bar{x})\mathbf{B}_i$, $\mathbf{N}_2(\bar{x}) = \mathbf{N}_{i,2}(\bar{x})\mathbf{B}_i$ and $\mathbf{D}(\bar{x}) = \mathbf{D}_i(\bar{x})\mathbf{B}_i$.

Using Eqs. (5), (6), (41)–(43), we have

$$\mathbf{u}_P = \begin{bmatrix} u \\ v \end{bmatrix} = \begin{bmatrix} \mathbf{N}_1\mathbf{p} - y\mathbf{D}\mathbf{p} - \frac{1}{2}\mathbf{p}^{\mathrm{T}}\mathbf{H}(\bar{x})\mathbf{p} \\ \mathbf{N}_2\mathbf{p} \end{bmatrix}, \tag{44}$$

where $\mathbf{H}(\bar{x})$ is the coupling shape function matrix which is an $3(n+1) \times 3(n+1)$ symmetry and non-negative define matrix, given by

$$\mathbf{H}(\bar{x}) = \mathbf{B}_i^{\mathrm{T}} \int_0^x \frac{\partial \mathbf{N}_{i,2}^{\mathrm{T}}}{\partial \bar{x}} \cdot \frac{\partial \mathbf{N}_{i,2}}{\partial \bar{x}}\, \mathrm{d}\bar{x}\mathbf{B}_i + \sum_{j=1}^{i-1} \left(\mathbf{B}_j^{\mathrm{T}} \int_0^{l_j} \frac{\partial \mathbf{N}_{j,2}^{\mathrm{T}}}{\partial \bar{x}} \cdot \frac{\partial \mathbf{N}_{j,2}}{\partial \bar{x}}\, \mathrm{d}\bar{x}\mathbf{B}_j \right). \tag{45}$$

Using the FEM with n element for the beam, the dynamic equation of the hub–beam system can be expressed as

$$\mathbf{M}\ddot{\mathbf{q}} = \mathbf{Q}, \tag{46}$$

where $\mathbf{q} = [\theta, \mathbf{p}^{\mathrm{T}}]^{\mathrm{T}}$ is the generalized coordinates of the hub–beam system; and $\mathbf{M}$ and $\mathbf{Q}$ are the generalized mass matrix and the generalized force matrix, respectively; given by

$$\mathbf{M} = \begin{bmatrix} M_{\theta\theta} & \mathbf{M}_{\theta p} \\ \mathbf{M}_{p\theta} & \mathbf{M}_{pp} \end{bmatrix},\ \mathbf{Q} = \begin{bmatrix} Q_\theta \\ \mathbf{Q}_p \end{bmatrix}, \tag{47}$$

where $M_{\theta\theta}$ is the rotary inertia of the system that is a scalar; $\mathbf{M}_{\theta p}$ and $\mathbf{M}_{p\theta}$ are $1 \times 3(n+1)$ and $3(n+1) \times 1$ inertia vectors caused by the nonlinear coupling between the rotating motion and the elastic deformation of the flexible beam; $\mathbf{M}_{pp}$ is an $3(n+1) \times 3(n+1)$ generalized elastic mass matrix; Q_θ is a scalar and $\mathbf{Q}_p$ is an $3(n+1) \times 1$ vector, both are generalized force parameters. All the parameters in Eq. (47) are given as follows

$$\begin{aligned} M_{\theta\theta} = {} & J_H + mR^2 + J_{11} + J_{22} + 2RE_1 + 2(R\mathbf{Y}_1 + \mathbf{Z}_{11})\mathbf{p} \\ & - \mathbf{p}^{\mathrm{T}}(R\mathbf{C} + \mathbf{D})\mathbf{p} + \mathbf{p}^{\mathrm{T}}\left(\mathbf{W}_{11} + \mathbf{W}_{22} + \overline{\mathbf{W}}_D\right)\mathbf{p}, \end{aligned} \tag{48}$$

$$\mathbf{M}_{p\theta} = \mathbf{M}_{\theta p}^T = \mathbf{R}\mathbf{Y}_2^T + (\mathbf{W}_{21} - \mathbf{W}_{12})\mathbf{p} + \mathbf{Z}_{12}^T + \overline{\mathbf{Y}}_D^T, \tag{49}$$

$$\mathbf{M}_{pp} = \mathbf{W}_{11} + \mathbf{W}_{22} + \overline{\mathbf{W}}_D, \tag{50}$$

$$\begin{aligned} Q_\theta = {} & -2\dot{\theta}\left[(R\mathbf{Y}_1 + \mathbf{Z}_{11})\dot{\mathbf{p}} - \mathbf{p}^{\mathrm{T}}(R\mathbf{C} + \mathbf{D})\dot{\mathbf{p}} + \mathbf{p}^E\left(\mathbf{W}_{11} + \mathbf{W}_{22} + \overline{\mathbf{W}}_D\right)\dot{\mathbf{p}}\right] \\ & - K_C\theta + \int_V \left[f_2\left(x + \mathbf{N}_1\mathbf{p} - y\mathbf{D}\mathbf{p} - \tfrac{1}{2}\mathbf{p}^{\mathrm{T}}\mathbf{H}\boldsymbol{p}\right) - f_1(y + \mathbf{N}_2\mathbf{p})\right] \mathrm{d}V, \end{aligned} \tag{51}$$

$$\begin{aligned} \mathbf{Q}_p = {} & -2\dot{\theta}(\mathbf{W}_{21} - \mathbf{W}_{12})\dot{\mathbf{p}} + \dot{\theta}^2\left(\mathbf{W}_{11} + \mathbf{W}_{22} + \overline{\mathbf{W}}_D\right)\mathbf{p} + \dot{\theta}^2(R\mathbf{Y}_1 + \mathbf{Z}_{11}) \\ & - \dot{\theta}^2(R\mathbf{C} + \mathbf{D})\mathbf{p} - \mathbf{K}_f\mathbf{p} + \int_V \left[f_1\left(\mathbf{N}_1^{\mathrm{T}} - y\mathbf{D}^{\mathrm{T}} - \mathbf{H}\mathbf{p}\right) + f_2\mathbf{N}_2^{\mathrm{T}}\right] \mathrm{d}V. \end{aligned} \tag{52}$$

The constant parameters in Eqs. (48)–(52) are given as follows

$$m = \rho AL, \tag{53}$$

$$E_1 = \int_V \rho x \, \mathrm{d}V = \frac{\rho AL^2}{2}, \tag{54}$$

$$J_{11} = \int_V \rho x^2 \, \mathrm{d}V = \frac{\rho AL^3}{3}, \tag{55}$$

$$J_{22} = \int_V \rho y^2 \, \mathrm{d}V = \rho LI, \tag{56}$$

$$\mathbf{W}_{jk} = \int_V \boldsymbol{\rho} \mathbf{N}_j^{\mathrm{T}} \mathbf{N}_k \, \mathrm{d}V = \sum_{i=1}^{n} \mathbf{B}_i^{\mathrm{T}} \int_0^{l_i} \rho A \mathbf{N}_{i,j}^{\mathrm{T}} \mathbf{N}_{i,k} \, \mathrm{d}\bar{x} \mathbf{B}_i \quad (j,k=1,2), \tag{57}$$

$$\overline{\mathbf{W}}_D = \int_V \rho y^2 \mathbf{D}^{\mathrm{T}} \mathbf{D} \, \mathrm{d}V = \sum_{i=1}^{n} \mathbf{B}_i^{\mathrm{T}} \int_0^{l_i} \rho I \mathbf{D}_i^{\mathrm{T}} \mathbf{D}_i \, \mathrm{d}\bar{x} \mathbf{B}_i, \tag{58}$$

$$\mathbf{Y}_k = \int_V \rho \mathbf{N}_k \, \mathrm{d}V = \sum_{i=1}^{n} \int_0^{l_i} \boldsymbol{\rho} A \mathbf{N}_{i,k} \, \mathrm{d}\bar{x} \mathbf{B}_i \quad (k=1,2), \tag{59}$$

$$\overline{\mathbf{Y}}_D = \int_V \rho y^2 \mathbf{D} \, \mathrm{d}V = \sum_{i=1}^{n} \int_0^{l_i} \rho I \mathbf{D}_i \, \mathrm{d}\bar{x} \mathbf{B}_i, \tag{60}$$

$$\mathbf{Z}_{1k} = \int_V \rho x \mathbf{N}_k \, \mathrm{d}V = \sum_{i=1}^{n} \int_0^{l_i} \rho A (x_i + \bar{x}) \mathbf{N}_{i,k} \, \mathrm{d}\bar{x} \mathbf{B}_i \quad (k=1,2), \tag{61}$$

$$\begin{aligned} \mathbf{C} &= \int_V \rho \mathbf{H} \, \mathrm{d}V = \sum_{i=1}^{n} \int_0^{l_i} \rho A \mathbf{H} \, \mathrm{d}\bar{x} \\ &= \sum_{i=1}^{n} \mathbf{B}_i^{\mathrm{T}} \int_0^{l_i} \int_0^{\bar{x}} \rho A \left(\frac{\partial \mathbf{N}_{i,2}^{\mathrm{T}}}{\partial \xi} \cdot \frac{\partial \mathbf{N}_{i,2}^{\mathrm{T}}}{\partial \xi} \right) \mathrm{d}\xi \, \mathrm{d}\bar{x} \mathbf{B}_i, \\ &\quad + \sum_{i=1}^{n} \sum_{j=1}^{i-1} \mathbf{B}_i^{\mathrm{T}} \int_0^{l_i} \int_0^{l_j} \rho A \left(\frac{\partial \mathbf{N}_{j,2}^{\mathrm{T}}}{\partial \xi} \cdot \frac{\partial \mathbf{N}_{j,2}^{\mathrm{T}}}{\partial \xi} \right) \mathrm{d}\xi \, \mathrm{d}\bar{x} \mathbf{B}_i, \end{aligned} \tag{62}$$

$$\begin{aligned} \mathbf{D} &= \int_V \rho x \mathbf{H} \, \mathrm{d}V = \sum_{i=1}^{n} \int_0^{l_i} \rho A (x_i + \bar{x}) \mathbf{H} \, \mathrm{d}\bar{x} \\ &= \sum_{i=1}^{n} \mathbf{B}_i^{\mathrm{T}} \int_0^{l_i} (x_i + \bar{x}) \int_0^{\bar{x}} \rho A \left(\frac{\partial \mathbf{N}_{i,2}^{\mathrm{T}}}{\partial \xi} \cdot \frac{\partial \mathbf{N}_{i,2}^{\mathrm{T}}}{\partial \xi} \right) \mathrm{d}\xi \, \mathrm{d}\bar{x} \boldsymbol{B}_i \\ &\quad + \sum_{i=1}^{n} \sum_{j=1}^{i-1} \mathbf{B}_i^{\mathrm{T}} \int_0^{l_i} (x_i + \bar{x}) \int_0^{l_j} \rho A \left(\frac{\partial \mathbf{N}_{j,2}^{\mathrm{T}}}{\partial \xi} \cdot \frac{\partial \mathbf{N}_{j,2}^{\mathrm{T}}}{\partial \xi} \right) \mathrm{d}\xi \, \mathrm{d}\bar{x} \mathbf{B}_i, \end{aligned} \tag{63}$$

$$\begin{aligned} \mathbf{K}_f &= \sum_{i=1}^{n} \mathbf{B}_i^{T} \int_0^{l_i} \left[EA \frac{\partial \mathbf{N}_{i,1}^{\mathrm{T}}}{\partial \bar{x}} \cdot \frac{\partial \mathbf{N}_{i,1}}{\partial \bar{x}} + EI \frac{\partial \mathbf{D}_i^{\mathrm{T}}}{\partial \bar{x}} \cdot \frac{\partial \mathbf{D}_i}{\partial \bar{x}} \right. \\ &\quad \left. + \mu GA \left(\mathbf{D}_i - \frac{\partial \mathbf{N}_{i,2}}{\partial \bar{x}} \right)^{\mathrm{T}} \left(\mathbf{D}_i - \frac{\partial \mathbf{N}_{i,2}}{\partial \bar{x}} \right) \right] \mathrm{d}\bar{x} \mathbf{B}_i. \end{aligned} \tag{64}$$

3. Numerical example

In this section, numerical simulation is carried out to demonstrate the effectiveness of the proposed dynamic model. Two cases, with and without considering the effect of shear deformation, are considered. The case with considering the shear deformation is namely the Timoshenko beam hypothesis. For this case the shear coefficient φ is considered in the modeling. The case without considering the shear deformation is the Euler–Bernoulli beam hypothesis, where $\varphi = 0$ is taken.

The material properties of the beam and structural parameters are given in Table 1. The hollow circular cross-section beam is adopted herein, where the length of the beam is $L = 2\,\mathrm{m}$, the inner radius $R_1 = 0.02\,\mathrm{m}$ and the outer radius $R_2 = 0.025\,\mathrm{m}$, as shown in Table 1. The equivalent diameter of the beam may be computed by $d_e = 2\sqrt{R_2^2 - R_1^2}$. Assume that the initial condition of the system is $\theta_0 = 30^\circ$ and $\dot{\theta}_0 = 0\,\mathrm{rad/s}$, and no external force is put on the system. Under this condition, the coiling spring is elongated and the system will behave with a free vibration. The elastic vibration of the beam will excite the large motion of the system, and the large motion of the system will affect the elastic vibration of the beam. These two motions act on each other. The shear coefficient of the cross-section of the beam, κ, is given by [18]

$$\kappa = \frac{6(R_1^2 + R_2^2)^2(1+\mu)^2}{7R_1^4 + 34R_1^2R_2^2 + 7R_2^4 + \mu(12R_1^4 + 48R_1^2R_2^2 + 12R_2^4) + \mu^2(4R_1^4 + 16R_1^2R_2^2 + 4R_2^4)}. \tag{65}$$

Under the initial condition, the time histories of tip response of the beam in y direction are shown in Fig. 4, where the solid line is the result using the Euler–Bernoulli beam hypothesis and the short dashed line the Timoshenko beam hypothesis. We can observe from Fig. 4 that the two results are overlapped. Fig. 5 is the amplitude–frequency result of the tip response of the beam in y direction using FFT. It is observed from Fig. 5

Table 1
The material properties and structural parameters

Length of the beam (L)	2 m
Density of beam material (ρ)	$3.0 \times 10^3\,\mathrm{kg/m^3}$
Inner radius of the beam (R_1)	0.02 m
Outer radius of the beam (R_2)	0.025 m
Young's modulus of beam material (E)	$7.27 \times 10^{10}\,\mathrm{N/m^2}$
Poisson's ratio of beam material (μ)	0.3
Rotary inertia of the hub (J_H)	$5\,\mathrm{kg\,m^2}$
Radius of the hub (R)	0.2 m
Stiffness of the coiling spring (k_C)	5000 N m/rad

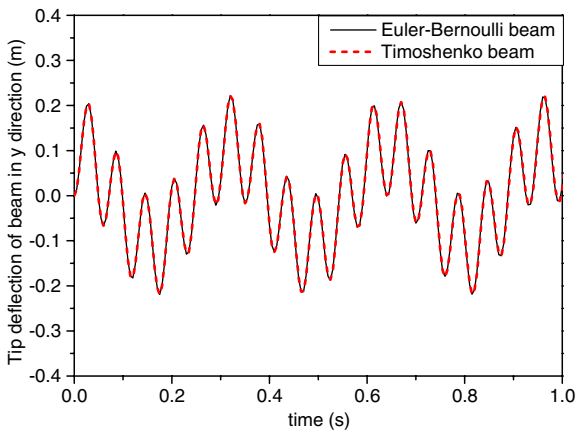

Fig. 4. The time history of tip response of the beam in y direction ($L = 2\,\mathrm{m}$).

that the response of the beam is mainly dominated by the first two modes. The first two vibration frequencies of the beam using the Timoshenko beam hypothesis are identical with those using the Euler–Bernoulli beam hypothesis, they are 3.125 and 17.188 Hz, respectively. Since the length of the beam is much larger than the

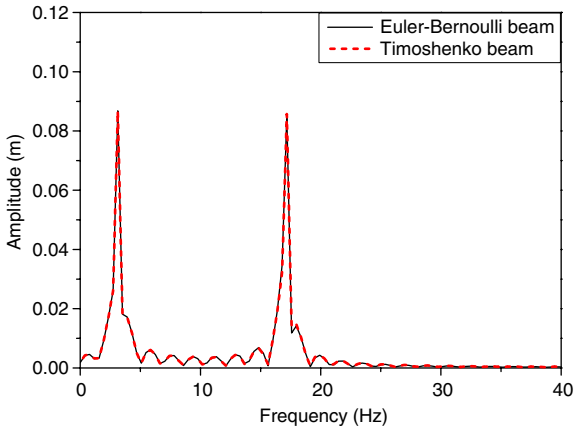

Fig. 5. Frequency–amplitude result of tip response of the beam in y direction ($L = 2$ m).

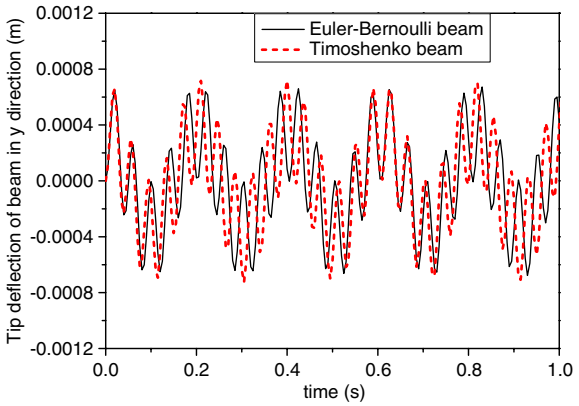

Fig. 6. The time history of tip response of the beam in y direction ($L = 0.5$ m).

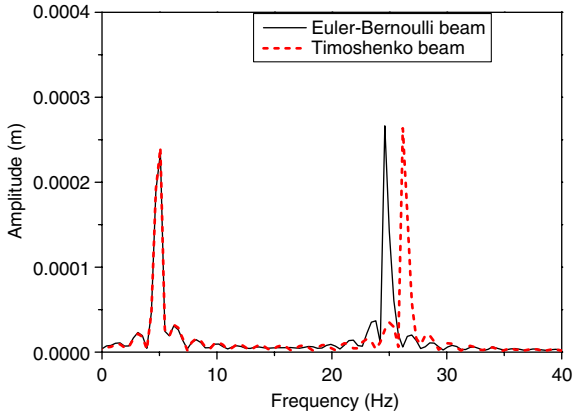

Fig. 7. Frequency–amplitude result of tip response of the beam in y direction ($L = 0.5$ m).

equivalent diameter of the beam for this case, φ has small effect on system dynamics that may be neglected. So the results using the Timoshenko beam hypothesis and the Euler–Bernoulli beam hypothesis are almost identical.

Next consider the case that the beam is short in length direction. The material properties of the beam and structural parameters are chosen to be the same as above except that the length of the beam is $L = 0.5\,\mathrm{m}$. The same initial condition of the system is taken, i.e., $\theta_0 = 30^\circ$ and $\dot{\theta}_0 = 0\,\mathrm{rad/s}$. In this case, the time histories of tip response of the beam in y direction and the amplitude–frequency results with and without considering φ are shown in Figs. 6 and 7, respectively. It is observed from Fig. 6 that there exists some difference in the two results. From Fig. 7, we can observe that the response of the beam is dominated by the first two modes. The first-order frequencies of the beam using the two hypothesis of flexible beam are identical, both are 5.078 Hz. But the second-order frequencies are different. It is 26.172 Hz using the Timoshenko beam hypothesis and 24.609 Hz using the Euler–Bernoulli beam hypothesis.

4. Concluding remark

In this paper, the coupling dynamic model of a hub–beam system with considering the shear deformation is investigated. The geometric stiffness term and the foreshortening quantity caused by the transverse deformation of beam are considered in the modeling. The dynamic model established using the Hamilton's principle is discretized using the FEM. The result using the Timoshenko beam hypothesis is compared with that using the Euler–Bernoulli beam hypothesis. Simulation results indicate that, when the ratio of length respect to the equivalent diameter of the beam is big, the effect of shear deformation of the beam on system dynamics is small and may be neglected in the modeling. But when the ratio is small, the shear deformation of the beam will have biggish effect on system dynamics and should be considered in the modeling. Whenever the ratio is big or small, the response of the beam is mainly dominated by the first two modes of the beam.

Acknowledgments

This research work is supported by the National Science Foundation of China (10372057, 10472065), the Shanghai Science Foundation (03ZR14062) and the "Shu Guang" Project of Shanghai (04SG16), for which the authors are grateful.

Reference

[1] J. Hong, L. Jiang, Flexible multibody dynamics with coupled rigid and deformation motion, *Advances in Mechanics* 30 (1) (2000) 15–20 (in Chinese).
[2] J. Hong, *Computational Dynamics of Multibody System*, High Education Press, Beijing, China, 1999 (in Chinese).
[3] T.R. Kane, R.R. Ryan, A.K. Banerjee, Dynamics of a cantilever beam attached to a moving base, *Journal of Guidance, Control and Dynamics* 10 (2) (1987) 139–150.
[4] J. Mayo, J. Dominguez, A.A. Shabana, Geometrically nonlinear formulation of beams in flexible multibody dynamics, *Journal of Vibration and Acoustics* 117 (1995) 501–509.
[5] I. Sharf, Geometric stiffening in multibody dynamics formulations, *Journal of Guidance, Control and Dynamics* 18 (4) (1995) 882–891.
[6] D.J. Zhang, R.L. Huston, On dynamic stiffening of flexible bodies having high angular velocity, *Mechanics of Structures and Machines* 24 (3) (1996) 313–329.
[7] J. Liu, J. Hong, Geometric stiffening of flexible link system with large overall motion, *Computers and Structures* 81 (2003) 2829–2841.
[8] J. Liu, J. Hong, Geometric stiffening effect on rigid–flexible coupling dynamics of an elastic beam, *Journal of Sound and Vibration* 278 (4–5) (2004) 1147–1162.
[9] G. Cai, J. Hong, X. Yang Simon, Dynamic analysis of a flexible hub–beam system with tip mass, *Mechanics Research Communications* 32 (2) (2005) 173–190.
[10] G. Cai, J. Hong, X. Yang Simon, Model study and active control of a rotating flexible cantilever beam, *International Journal of Mechanical Sciences* 46 (6) (2004) 871–889.
[11] H. Yang, J. Hong, Z. Yu, Dynamics modeling of a flexible hub–beam system with a tip mass, *Journal of Sound and Vibration* 266 (4) (2003) 759–774.
[12] H. Yang, Study of Dynamic Modeling Theory and Experiments for Rigid–Flexible Coupling Systems. PhD Dissertation, Shanghai Jiaotong University, China, 2002 (in Chinese).

[13] H. Yang, J. Hong, Z. Yu, Vibration analysis and experiment investigation for a typical rigid–flexible coupled system, *Chinese Journal of Astronautics* 23 (2) (2002) 67–72 (in Chinese).
[14] H. Yang, J. Hong, Z. Yu, Experiment validation on modeling theory for rigid–flexible coupling systems, *Acta Mechanica Sinica* 35 (2) (2003) 253–256 (in Chinese).
[15] X. Tong, B. Tabarrok, K.Y. Yeh, Vibration analysis of Timoshenko beams with non-homogeneity and varying cross-section, *Journal of Sound and Vibration* 186 (5) (1995) 821–835.
[17] J. Cao, *Study on Stochastic Eigen-problems of Vibrational Systems*, Master Dissertation in Shanghai Jiaotong University, China, 2000 (in Chinese).
[18] J.R. Hutchinson, Shear coefficients for Timoshenko beam theory, *ASME Journal of Applied Mechanics* 68 (2001) 87–92.